

Spatial prediction of soil erosion risk by RUSLE model and geospatial tools in Ouljet Sultane watershed (Central Morocco)

Prédiction spatiale du risque d'érosion du sol par le modèle RUSLE et les outils géospatiaux dans le bassin versant d'Ouljet Sultane (Maroc- Central)

Nassima MOUTAOIKIL¹, Mohamed MASTERE^{1,2*}, Brahim BENZOUAGH^{1,3}, Bouchta EL FELLAH¹, Hind LAMRANI¹, Mohammed EL BRAHIMI¹, Driss SADKAOUÏ⁴

1. Department of Geomorphology and Geomatics, Scientific Institute, Mohammed V University in Rabat, Avenue Ibn Battouta, Agdal, P.B 703, 10106 Rabat-City, Morocco. (nassimamoutaouikil@gmail.com).
2. School of Public Management, Governance and Public Policy, College of Business & Economics, University of Johannesburg, South Africa.
3. Laboratory of Geoenvironment and Environment, Cartography and Tectonophysics team (CaTec), Department of Geology, Faculty of Sciences, Moulay Ismail University, Meknes, Morocco.
4. Department of Geology, Laboratory: Environmental Geology and Natural Resources, Faculty of Sciences, Abdelmlek Essaâdi University, Tetouan, Morocco.

Abstract. Soil erosion is a major environmental issue worldwide, posing significant threats to land productivity and ecosystem stability. In the Ouljet Sultane watershed, the main environmental concern is the risk of soil erosion. This research aims to use the Revised Universal Soil Loss Equation (RUSLE) model to estimate annual soil loss in the region and assess the relative contributions of erosion-regulating factors. The GIS environment incorporates model variables such as soil erodibility (K), rainfall erosivity (R), topography (LS), land cover and management (C), and support practices (P). A layer was developed for each of these components, and the GIS calculator was used to multiply the raster values of each parameter. According to the RUSLE model and GIS raster calculations, soil erosion occurs at an average rate of 22.5 t/ha/year. Rainfall has been identified as the most sensitive factor influencing soil erosion risk in the sub-catchment area. Soil erosion estimates indicate that immediate intervention is necessary to mitigate soil loss. However, to develop effective conservation measures, further research is needed on erosion severity, area prioritization, and sediment loss projections in this watershed.

Keywords: Soil Loss, Ouljet Sultane Basin, Water Erosion, RUSLE Approach, GIS and Remote Sensing, Morocco.

Résumé. Le problème environnemental le plus complexe dans le bassin versant d'Ouljet Sultane est le risque d'érosion des sols. Par conséquent, cette étude vise à utiliser le modèle Equation Universelle Révisée des Pertes en Sol (RUSLE) pour calculer les pertes en sols annuelle dans le bassin versant et évaluer les contributions relatives des facteurs de régulation de l'érosion. L'environnement SIG comprend des variables de modèle telles que l'érodibilité du sol (K), l'agressivité des pluies (R), la topographie (LS), la gestion et la couverture (C), et les pratiques de soutien (P). Une couche SIG (layer) a été développée pour chacun de ces composants. Le calculateur SIG a été utilisé pour multiplier les valeurs raster de chacun de ces paramètres. L'érosion des sols se produit à un taux moyen de 22,5 t/h/an, comme déterminé par le modèle RUSLE et les calculs de grille SIG. Les précipitations se sont avérées être l'élément le plus sensible influençant le risque d'érosion des sols dans la région du sous-bassin versant. Les estimations de l'érosion des sols indiquent qu'une intervention immédiate est nécessaire dans la région pour protéger le sol. Cependant, pour créer des mesures de conservation efficaces, une enquête plus approfondie est nécessaire sur les évaluations de la gravité de ce bassin versant, la hiérarchisation des zones et la projection des pertes en sédiments.

Mots clés : Perte de sol, Bassin d'Ouljet Sultane, Érosion hydrique, Approche RUSLE, SIG et télédétection, Maroc.

INTRODUCTION

One of the difficult problems of the twenty-first century is land degradation (Ezzaouini *et al.* 2020, Hara *et al.* 2021, Sands 2023, Benzougagh *et al.* 2024). The global sustainability of natural resources, land management, ecosystem health, and agricultural production are all impacted by soil erosion risk, this poses a significant risk to the environment (Batist *et al.* 2019, Brahim *et al.* 2020, Bammou *et al.* 2024). Significant environmental issues are brought on by sediment export to rivers and lakes and soil erosion. Various types of land degradation, including salinization, compaction, acidity, soil sealing, soil erosion, soil pollution, and desertification, affect more than 6 billion hectares globally (Ganasri & Rameh. 206, Ganzour *et al.* 2024, Bezak *et al.* 2024). Unchecked

soil erosion and the resulting land degradation have rendered large expanses of land economically useless in many areas. Consequently, agricultural systems lost 75 billion tons of rich soil annually. (Sarapatka *et al.* 2019, Phinzi *et al.* 2021).

Monitoring soil erosion risk is crucial for effective land protection. However, assessing soil erosion using experimental plots may be costly and time-consuming. Around the world, several techniques have been developed and implemented for evaluating soil erosion. For many years, scientists have been simulating soil erosion. There are over 82 models of soil erosion that employ different methods and approaches (Brahim *et al.* 2020, Bezak *et al.* 2024) among these are the Morgan-Morgan-Finney (MMF) (Morgan *et al.* 1984) The European Soil Erosion Model (EUROSEM) (Morgn 2001),

the Water Erosion Prediction Project (WEPP) (Nearing *et al.* 1997), the Universal Soil Loss Equation (USLE) (Wischmeier & Smith 1965, 1978) and its updated version, RUSLE (Renard *et al.* 1991); EPM (Gavrilovic 1962); are among the tools that researchers and policymakers frequently use. The Water and Tillage Erosion Model, the Sediment Delivery Model (WaTEM/SEDEM) (Van Oost *et al.* 2000); STREAM (Cerdan *et al.* 2002); the Soil and Water Assessment Tool (SWAT) model (Arnold *et al.* 2012); distributed soil erosion and sediment yield model (DSESYM) (Yuan *et al.* 2015). Of these, the RUSLE model is thought to be one of the empirical models used most frequently to evaluate soil water erosion.

Water erosion is a significant problem in Morocco, presenting various challenges to the country. Factors such as irregular and intense precipitation, steep slopes, deforestation, intensive agriculture, and inadequate land management practices contribute to the risk of soil erosion (Chadli 2016, Moussi *et al.* 2023). Ecosystems are damaged, fertile soil is lost, water retention capacity is reduced, and agricultural output is lowered as a result of this erosion. It also impacts water resources, water quality, and infrastructure stability (Benzougagh *et al.* 2022, Sadkaoui *et al.* 2023, Bammou *et al.* 2024). Nevertheless, a number of factors, including intense rainstorms, steep hills, deforestation, burning plant cover, insufficient land management techniques, and unsustainable farming methods, were essential in hastening the depletion of soil water. Therefore, the purpose of this study was to determine the borders of the soil erosion risk zone and forecast soil loss using the RUSLE model. Utilizing the Geographic Information Systems (GIS)-based model estimate, a second computation of the possible soil erosion's geographic distribution within the study area. The RUSLE model uses several criteria to estimate soil erosion: runoff erosivity (R), soil erodibility (K), slope steepness (S) and slope length (L), cover and management techniques (C), rainfall, and support for conservation initiatives (P) (Renard & Freimund 1994). Therefore, the data acquired from this study will be helpful in creating strategies for managing soil erosion in the study region, assisting planners, soil scientists, and policymakers. To address this issue, implementing soil conservation measures, adopting sustainable agricultural practices, and raising awareness among stakeholders are crucial. Additionally, research, monitoring, and capacity-building initiatives can assist in the creation of efficient erosion control plans adapted to Morocco's various areas. By addressing water erosion, Morocco can protect its agricultural lands, preserve natural ecosystems, and ensure the sustainability of its water resources.

MATERIALS AND METHODS

Study area

Beht watershed, which contains two dams, the upstream El Kansera Dam, and the central Ouljet Sultane Dam has a surface area of 6196.26 km². The research area is shaped like an extended rectangle with its NW-SE orientation. The cities of Sidi Kacem and Sidi Slimane border it to the north; Meknes borders it to the northeast; El Hajeb, Ifrane, and Jbel Hebri border it to the east; Mrirt and Oued Oum Rabia border it to the south; and Oulmes and Khemisset border it to the west.

With features including depressions, multibranched gullies, extraordinarily high rocky outcrops, and alluvial terraces serving as accumulation forms, the research region's terrain ranges from being comparatively flat to being somewhat rocky. With a height range of 299 to 2134 meters, the steep slopes encompass around thirty percent of the watershed area.

A sub-basin of the Oued Sebou is the Oued Beht hydrographic basin. Watercourses of this river originate in the northern central region of Morocco and the western Middle Atlas. It joins the lower Oued Sebou after crossing the central Rif southern trench, where it receives contributions from a number of significant tributaries, then the southern portion of the El Gharb plain and the Pre-Rif, which is part of the western central Rif southern trench (Fig.1).

Research region consists of an anticlinal dome of tectono-diapiric origin separating two synclinal depressions. Previous studies examined the spatial and temporal variations of various sedimentary units' deposit typology and contemporary sediment dynamics (Laabidi *et al.* 2017). The morpho-structural conditions of the valley, which have a significant impact on the typology of the fluvial styles, are connected to the morpho-sedimentary typology of the study area's fluvial sedimentary settings as well as their spatial distribution and history (Ait Yacine *et al.* 2019). The meandering style with anastomosed tendency and the straight to weakly sinuous style with braid tendency are, in fact, the most popular fluvial styles. The first type originated in the present-day riverbed, which is made up of fragile clayey and swampy Miocene and Triassic era terrain. The valley is large and divided into depressions with synclinal structure. In the second kind, Jurassic carbonate terrains cause the valley to narrow and form an anticlinal dome.

In terms of geology, the study area includes formations from the Quaternary to the Paleozoic. The geological formations of the Paleozoic basement and cover dip beneath Upper Miocene formations in the central Rif southern trench. The Miocene formations are unconformably overlain by the deposits of the fluvial terraces of the Oued Beht, which are stratified and nested (Michard 1976, Fedan 1988, Capella *et al.* 2017). The watershed is situated on three geological and structural domains: the Hercynian Central Morocco (Beaudet 1969, Sabaoui 1987, Saidi *et al.* 2020), the southern Rif trench and the Middle Atlas Causse. It is entirely established on the impermeable formations of the Primary and Permo-Triassic of the Central Massif. The Quaternary basalts over which the Oued Beht flows at its source are of little significance to be considered (Marghich 1988, Lakhili *et al.* 2021). In the vast Paleozoic complex, of Ordovician, Silurian, and Carboniferous age, shales make up the bulk of the formations and sometimes show intercalations of quartzites and limestones, (Fig. 2). Further north, but upstream of El Kansera, the red saline clays of the Permo-Triassic appear, associated with a few limited extent basalts (Lakhili 2018).

The watershed features a diversity of soils that significantly influence its hydrological processes and capacity to support vegetation (Lakhili 2018, Ait Yacine *et al.* 2019). This variety is linked to the geology, climate, and human activities in the region. The main types of soils found in the watershed are: (i) Clay soils: Composed of fine particles, these soils have excellent water retention capacity. They are often located in low-lying areas and depressions of the watershed. However, their dense structure makes them susceptible to compaction, which can limit water infiltration and plant rooting. (ii) Sandy soils: Made up of coarse particles, sandy soils provide exceptional drainage. They are generally found at higher elevations or in well-drained areas. Nevertheless, their low water and nutrient retention capacity limits their natural fertility. (iii) Loamy soils: Considered the most balanced, these soils have an optimal mixture of sand, silt, and clay. They offer good drainage while retaining enough water and nutrients for plant growth. Loamy soils are often found in floodplains and along riverbanks. (iv) Saline soils:

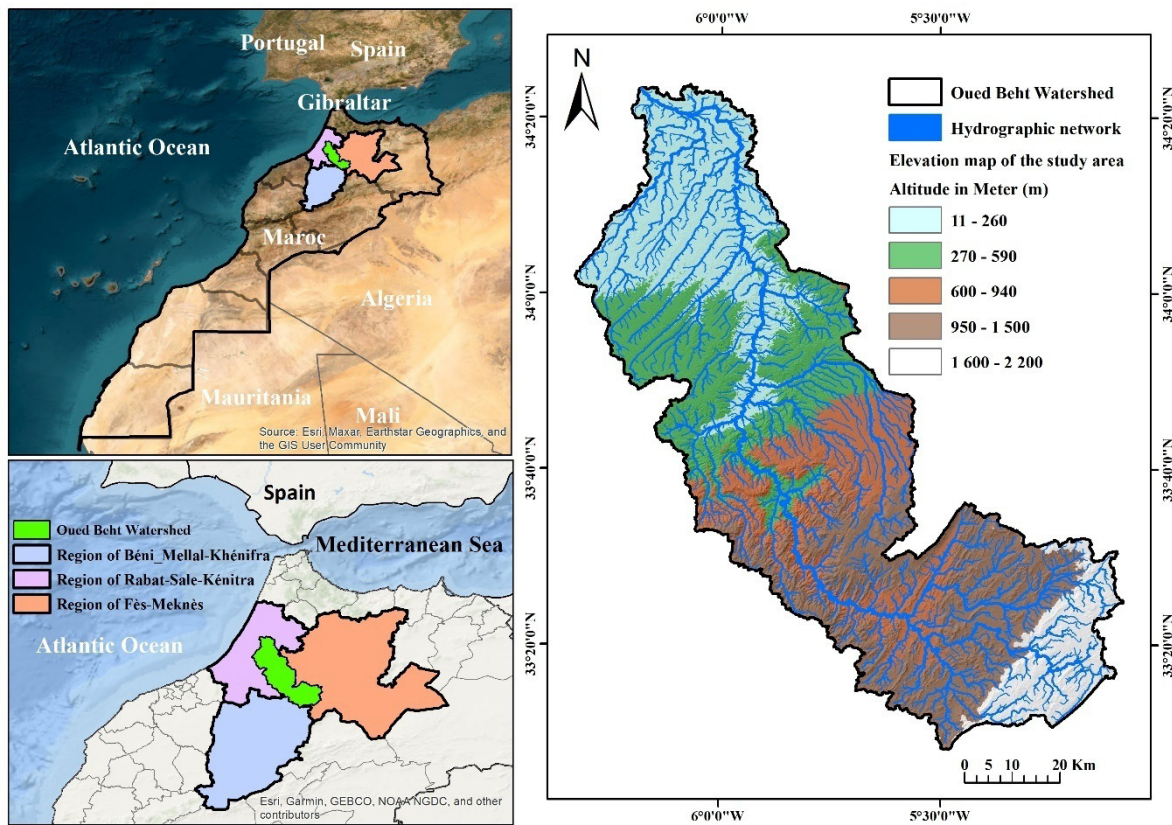


Figure 1. Location map of the Ouljet Sultane watershed.

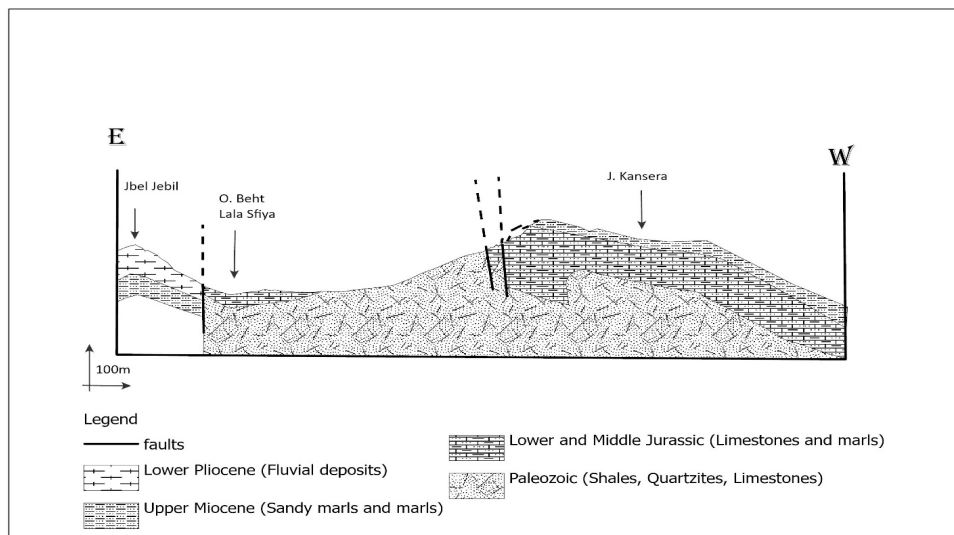


Figure 2. Geological section of study area.

Characterized by a high concentration of salts, these soils are frequently found in arid or semi-arid regions, as well as in coastal areas. Salinity limits plant development by disrupting physiological processes. (v) Organic soils: Rich in organic matter, these soils form in wetland areas, such as peat bogs and marshes. They play a crucial role in the carbon cycle and harbor specific biodiversity.

Knowledge of soil types is a fundamental element in assessing the risk of water erosion using the RUSLE (Universal Soil Loss Equation) model. Indeed, the K factor in this equation represents the soil erodibility, which indicates its sensitivity to erosion.

The Atlantic Ocean and the Saharan domain, which are situated in the west and east of northern Morocco, both have an impact on the Mediterranean climate that prevails in the Beht basin (Nastos *et al.* 2013). An average of 700 mm of precipitation falls on the basin each year, with variations varying from 1000 mm in the wet northern Middle Atlas to 400 mm in the high Beht valley. The amount of rain that falls throughout the year is not uniform and fluctuates greatly from year to year and month to month. These rains often occur in the form of thunderstorms and are characterized by occasionally violent floods (Benzougagh *et al.* 2021).

METHODOLOGY

RUSLE model structure

Renard *et al.* (1997) developed RUSLE model to assess how physical and anthropogenic variables, Raindrops and surface runoff cause soil erosion at the rill and inter-rill scales, which is affected by elements including land use and cover. RUSLE is a commonly used global approach for calculating the rates of long-term deterioration in field otherwise farm-sized units under varied management strategies. The results of this model provide important insights for soil conservation and sustainable land management strategies by allowing researchers and land managers to assess the potential impact of various land use and management scenarios on soil erosion. Its widespread global use demonstrates its usefulness in calculating and predicting rate of soil erosion, assisting in the development of erosion control methods, and making knowledgeable choices on agriculture methods and land use planning. As this study utilized the RUSLE model (Fig. 3), five parameters were assessed, and the average annual soil loss over the long run was determined (Eq.1).

$$A = R \times K \times LS \times C \times P \text{ (Eq.1)}$$

Where:

A: soil erosion rate or average annual soil loss due to sheet and rill erosion (t/ha/y);

R: factor that determines how erosive rainfall is, explaining the strength and duration of storms(mm/ha/h/y);

K: erodibility factor, which gauges how easily soil may separate under typical circumstances (t. ha/MJ.mm);

LS: steepness and length of the slope (L in m and S in %);

C: factor for management cover those accounts for surface roughness, canopy, surface cover, and the effects of past land usage;

P: support factors technique.

The following explains each variable that impacts the rate of erosion based on the erosion estimate equation mentioned above:

Rainfall Erosivity Factor (R)

Rainstorm intensity and duration can impact soil stability, particularly when they surpass soil resistance, leading to increased erosion (Ollobarren Del Barrio *et al.* 2018, Brahim *et al.* 2020). The amount of soil detachment brought on by raindrop splash erosion at a certain place is reflected in the rainfall erosivity factor (mm/h/y). The product of rainfall kinetic energy (E) and maximum 30-minute rainfall intensity (I₃₀) continuous precipitation data is used to compute the R factor (Wischmeier & Smith 1978, Ganasri & Ramesh 2016). However, in addition to flawed data collection procedures, it is difficult to get rain gauge-based data on rainfall intensity over extended in the research region. Researchers have proposed simplified techniques for calculating rainfall erosivity using monthly and yearly rainfall (da Silva 2004, Dutta *et al.* 2019). Utilizing information from rain gauge stations dispersed around the research region, as well as riparian zones, spatial variations in precipitation can be taken into account. This provides a comprehensive and more detailed map of regional rainfall patterns (Fig. 4).

According to Arsyad (2010), the value of R indicates the erosive capacity of rainfall at a particular place or the erosivity of yearly rainfall. Other formulas exist for calculating the R factor; however, for the sake of this study, Lenvain's (1975) formula, presented in equation (Eq. 2), was used. Some formulas are more complex than others. Lenvain's formula might have been preferred due to its simplicity and ease of calculation (data availability) for the study area.

$$R = 2.21 \times P^{1.36} \text{ (Eq.2)}$$

Where: R is the factor of rainfall erosivity(unit/month); P is the monthly average rainfall (cm).

The choice of interpolation method for estimating the R factor in the study area is influenced by the spatial distribution of available rainfall data. This study employs Kriging as the interpolation technique. Kriging is a geostatistical method that accounts for spatial autocorrelation in the data, yielding more precise interpolations, especially for datasets exhibiting strong spatial structures.

Soil Erodibility Factor (K)

Soil erodibility (K) reflects the soil's susceptibility to erosion, or how quickly it erodes (Arsyad 2010). The soil's organic and chemical content, infiltration capacity, soil texture, and soil aggregate stability all affect how erodible the soil is (Mastere *et al.* 2013, Brahim *et al.* 2020, Faouzi *et al.* 2023). Fu *et al.* (2011) and Millward and Mersey (1999) assert that it explains why the soil reacts over time to periods of intensely erosive precipitation. Soil erodibility as influenced by soil parameters is measured by factor (K). Wischmeier and Smith (1978) presented a straightforward technique for calculating the erodibility factor that considers five soil properties: permeability, sand, silt, soil structure, and percent organic matter (OM). According to Yitayew *et al.* (1999), Ouallali *et al.* (2016), Hara *et al.* (2021) and Brahim *et al.* (2020), The most effective techniques for evaluating soil properties as factors influencing erodibility of soil, are field testing. K is a measure of the susceptibility of soil particles to detachment and transport by rainfall and runoff. Texture is the principal factor affecting K, but structure, organic matter and permeability also contribute (Stone & Hilborn 2012).

To build a vector coverage map, some researchers scan pre-existing soil maps that may be obtained in hard copy format from government agencies. The FAO soil classification system or the Agricultural Handbook (Shamshad *et al.* 2008) are two sources that are used to classify the soils (Millward & Mersey 1999, El Brahimi *et al.* 2022). Vector soil map was then converted using ArcGIS tools to produce a raster map. In their investigation of Morocco's Oued Amter watershed, El Brahimi *et al.* (2022) computed soil loss from agriculture using the RUSLE and GIS methodologies. El Brahimi *et al.* (2022) created the soil map of the Oued Amter watershed, and their findings show that the watershed has very thin sandy and silt loam soil textures, as well as a high soil erodibility of about 88.9%. The soil map is used to calculate the soil erodibility factor for the watershed. Interpretation of the soil characteristics of the target area allowed them to be classified in the Wischmeier and Smith (1978) chart to approximate the K-factor based on the parameters of organic matter, structure, texture, and permeability. Determination of these parameters is difficult due to the lack of a soil survey in the study area. The K factor is a determining factor in the equation of Wischmeier and Smith (1978) (Eq.3) since it reflects the degree of erodibility of soils through the determination of their composition. Thus, its estimation was based on the analysis of soil samples taken in the study area by applying the following equation (Eq.3):

$$100K = 2.1M^{1.14} \times 10^{(-4)} (12-a) + 3.25(b-2) + 2.5(C-3) \text{ (Eq.3)}$$

Where:

K: Soil erodibility in ha.H/ha.MJ.mm; **M:** (% Fine sand + % Silt) *(100-% Clay); **a:** % of organic matter; **b:** Soil structure code (1 to 4) [1: Very fine; 2: Fine; 3: Medium and coarse; 4: very coarse]; **c:** Permeability code (1 to 6) [1: Fast; 2: Medium to fast; 3: Moderate; 4: Slow to moderate; 5: Slow and 6: Very slow].

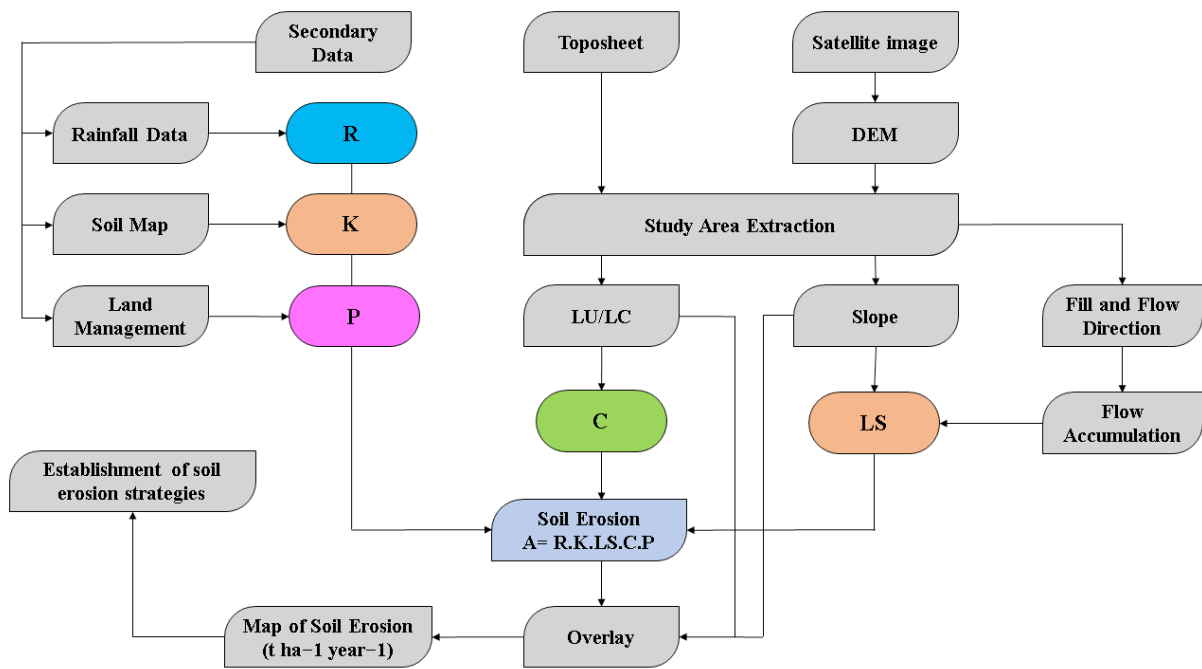


Figure 3. Flow chart of methodology.

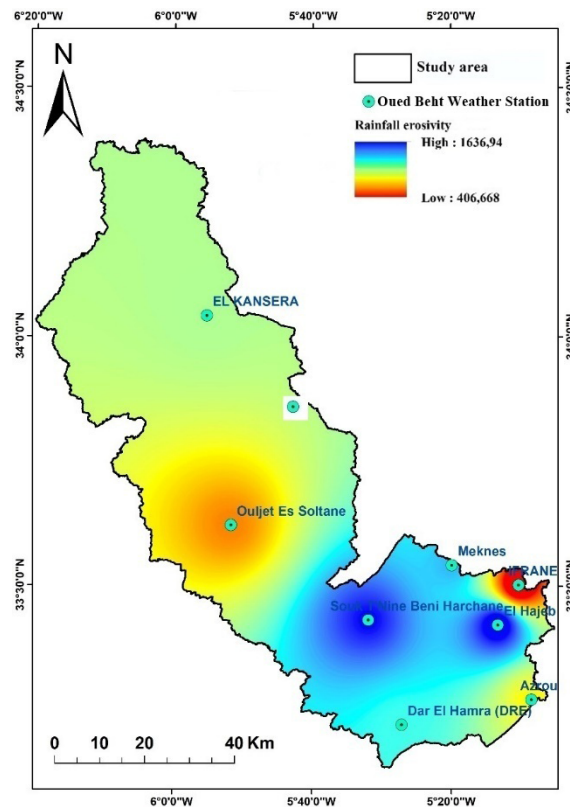


Figure 4. Spatial distribution of rainfall stations in the study area.

Slope Length and Steepness Factor (LS)

The RUSLE model's Length and Slope component explains how topography affects erosion. Experts in soil erosion used to define slope length as the distance between the onset of overland flow and the point at which the flow concentrates in a specific channel or the slope gradient decreases to a level where deposition may begin (Wischmeier & Smith 1978, Römken *et al.* 1995, Renard *et al.* 1997). Haan *et al.* (1994) found that increased water velocity causes

erosion to increase proportionately with slope length. As a result, soil loss rises in proportion to length slope and gradient (McCool *et al.* 1987). A trustworthy estimate the impacts of slope length and inclination are combined to generate the rate of soil erosion. The two most prevalent forms of erosion are inter-rill and rill. Surface runoff that follows the direction of the slope causes inter-rill erosion. The impact of raindrops striking the ground is what causes the latter. Although it does

not distinguish between the two forms of erosion, the RUSLE depicts both of them.

Several researchers have used the basic technique of determining the topographic influence on erosion by combining both components (L and S). With GIS technology, many academics now use DEMs to generate topographical data. Contours that are digitally digitized and have set intervals are used to build the DEM (30 m). There are several topographical calculation formulas. Numerous investigators have employed the methodology suggested by Stone and Hilborn (2012). Equation (Eq.4) illustrates that this method requires steeper slopes and flow accumulation.

$$LS = (\text{Flow accumulation} \times \text{Cell size}/22,13)^{0.4}(\sin(\text{Slope})/0.0896)^{1.3} \text{ (Eq.4)}$$

Where: The complete flow accumulated in each cell on a frame basis, weighted for all cells flowing into each downstream cell, is represented by the flow accumulation map); grid cell size: the size of the grid cell determined by using the 30 m resolution of the DTM; slope length and steepness factor (LS); The gradient: a degree-by-degree slope chart.

Management of the vegetation cover: factor (C)

The way that ground cover—whether it originates from grass and trees in non-agricultural settings or crops in agricultural environments and the associated management techniques to reduce soil loss—affects soil cover may be clarified through controlling the quantity of vegetation component (Renard *et al.* 1997). When vegetation grows, soil loss decreases because ground cover tends to lessen the erosive power of raindrops before they reach the soil’s surface (Jahun *et al.* 2015, Benzougagh *et al.* 2022). In order to reduce erosion and runoff rates, several forms of crop cover as well as plant cover are essential. An effective way to decrease soil erosion is to manage plants and plant wastes (Lee 2004, Bammou *et al.* 2024). In their assessment research of refined surfaces in decreasing erosion (Benkobi *et al.* 1994), state that steepness, slope length, and surface cover are important variables in regulating soil loss.

The C-factor can be computed using a variety of techniques: (i) Historically, surface cover factor has been determined using empirical estimates derived from

observations of various parameters associated with ground cover gathered from model plots. (ii) Weighted average soil loss ratios (SLRs), which are calculated by accounting for several sub-factors like surface roughness, canopy cover, prior land use, and surface cover, can also be used to create it (Renard *et al.* 1991, Chadli 2016). (iii) The method that is now most frequently used to calculate the surface cover factor is the classification of cover land and land use from satellite images using remote sensing techniques (iv) One of the most often used methods in remote sensing to calculate the C factor is the Normalized Difference Vegetation Index, or NDVI. This index, it is obtained from equation (Eq.5) for Landsat-8 images and is used in the current work to evaluate surface cover types.

$$NDVI = (NIR - R) / (NIR + R) \text{ (Eq.5)}$$

Where: NDVI is the normalized difference vegetation index; NIR is the near-infrared band reflectance; R is the red band reflectance.

Higher values indicate healthier and denser vegetation. The range of NDVI values is -1 to 1. Water bodies or places devoid of vegetation are indicated by values near to -1, whereas thick and vigorous vegetation is indicated by values near to 1. Studies (Kriegler *et al.* 1969), additionally demonstrated that crop type and management techniques have an impact on the slope values that are projected for arable land (Eq.6).

$$C = e^{-\alpha((NDVI)^\beta - NDVI)} \text{ (Eq.6)}$$

Where: α and β are unitless parameters that determine the shape of the curve relating to NDVI and C factor.

The RUSLE Fact Sheet from Ontario’s Ministry of Agriculture, Food, and Rural Affairs in Canada and the Erosion and Sediment Control Manual from Georgia’s Soil Water and Conservation Commission in 2000 were the sources of the C factor (Tab.1) values for each kind of land use.

Soil Conservation Practice Factor (P)

A dimensionless ratio called the conservation and management practice factor (P) considers soil loss as a consequence of certain management strategies into consideration (Wischmeier & Smith 1978, Renard *et al.* 1997). It offers an illustration of how lowering the volume

Table 1. Values of the C-factor.

Land use class	C-factor
Rainfed agricultural lands	0.07
Mosaic agriculture (20–50%) and vegetation (20–70%) (grassland, shrubland, and forest)	0.07
Mosaic vegetation: 20–50% agriculture and 50–70% grassland, shrubland, and forest	0.1
Closed (>40%) deciduous woodland with wide leaves (>5 m)	0.001
Closed (>40%) evergreen needleleaf forest (>5 m)	0.001
Closed to open (>15%) mixed woodland with needle- and broad-leaved leaves (>5 m)	0.001
Mosaic woodland or shrubland (between 20 and 50 percent) or shrubland	0.1
Mosaic shrubland or woodland (20–50%), or grassland (50–70%)	0.1
Closed to open ([15 %] shrubland (<5 m) with broadleaved or needle-leaved evergreen or deciduous leaves.	0.001
Very little (<15%) vegetation	0
Artificial surfaces and their surroundings (almost 50% of urban areas)	0
Bare regions	0
Bodies of water	0

and velocity of water flow might lessen erosion. The P-factor is the ratio of soil loss from a support technique to that from straight-row farming that is done up and down. Stone and Hilborn (2012) found that the most widely used farming techniques were contour farming, cross-slope farming, and strip cropping.

P values increase when agricultural producers plow vertically without conservation measures. But when conservation measures are used, the P-value usually goes down. The P factor was derived from Table 2 for the US and Canada and the Glob cover map, using a method similar to that used for the C factor.

Table 2. Values of P-factor (Chadli 2016).

Land use class	P-factor
Rainfed croplands	0.5
Rainfed agricultural lands	0.5
Mosaic agriculture (20–50%) and vegetation (20–70%) (grassland, shrubland, and forest)	1
Mosaic vegetation: 20–50% agriculture and 50–70% grassland, shrubland, and forest	1
Closed (>40%) deciduous woodland with wide leaves (>5 m)	1
Closed (>40%) evergreen needleleaf forest (>5 m)	1
Closed to open (>15%) mixed woodland with needle- and broad-leaved leaves (>5 m)	1
Mosaic woodland or shrubland (between 20 and 50 percent) or shrubland	1
Mosaic shrubland or woodland (20–50%), or grassland (50–70%)	1
Closed to open ([15 %] shrubland (<5 m) with broadleaved or needle-leaved evergreen or deciduous leaves.	1
Very little (<15%) vegetation	1
Artificial surfaces and their surroundings (almost 50% of urban areas)	1
bare regions	1
bodies of water	1

RESULTS

Factors Controlling Soil Erosion

The rainfall research of the eight meteorological stations revealed irregularity of precipitation in space and time. The rainfall erosion factor (R) ranges from 157 to 1981 MJ mm/h/y. The eastern portion of the watershed has the highest values, while the center region has intermediate readings. The northeastern part of the catchment has lower values, with a poor distribution (Fig. 5a). The soil erodibility factor (K) has a range of values from 0.119 to 0.162 t ha h ha⁻¹ MJ⁻¹ mm⁻¹ (Fig. 5b). Soils with low antecedent moisture content and high permeability are associated with lower K-factor values, and low water content. A topographic indicator that depicts the shape of the terrain is the LS-factor. To calculate the slope, a 12.5-meter-resolution digital elevation model (DEM) was employed. The LS-factor results for the whole watershed varied from 2.5 to 59.5 (Fig. 5c). The majority of the land within the classes is characterized by low slopes, which account for roughly half of the total basin area. Twenty percent of the watershed is made up of medium-slope terrain, mostly in the median and a few locations upstream and downstream. Only 10% of the entire region under investigation is made up of areas has incredibly steep slopes that are situated in the center of the watershed. The Cover Management Factor (C) has a range of values from 0 to 1 (Wischmeier and Smith 1978). The C factor represents the effect of plant cover on soil loss. A value of 0 indicates complete cover, while a value of 1 indicates bare soil. The spatial distribution of the Cover Management Factor (C) within the study area, as depicted in Figure 5d, exhibited values ranging from 0.21 to 0.59 (Fig. 5d).

Potential Erosion Risk Analysis

The RUSLE model parameters for rainfall erosivity (R), soil characteristics (K), topography (LS), cover management

(C), and requirements for conservation and management techniques (P) were used to create a future erosion risk map for the Ouljet Sultane watershed. The potential soil erosion map (map of A factor) of Ouljet Sultane has been developed in the GIS application through the five components' multiplication (R, K, LS, C, and P). Using the categorization scheme created by the United Nations Food and Agriculture Organization (FAO) in 1979 (Tab.3), there were five categories on the risk map (Fig.6) for the succeeding soil erosion, between extremely low and extremely high risk. The characteristics of surface cover and slope have distinct implications on the possibility of soil erosion risk. These factors combine to determine the degree of risk in Ouljet Sultane watershed. Steeper slopes often represent a higher danger of erosion, landslides, or runoff, especially in combination with inadequate surface cover such as plant or protective barriers. On the other hand, regions with gradual slopes and appropriate surface cover may be less susceptible to such risks. When analyzing and managing hazards in a variety of contexts such as land management, infrastructure development, and natural disaster preparedness, slope and surface cover must be taken into account. 97% of the study area has a low erosion risk, according to the data, 0.85% has a medium risk, and 1.78 percent has a high risk.

Table 3. Erosion risk classification (FAO 1979).

Erosion rate in t/ha/y	Risk class
200<	Very high
200 - 50	High
50 - 10	Medium
10 >	Low

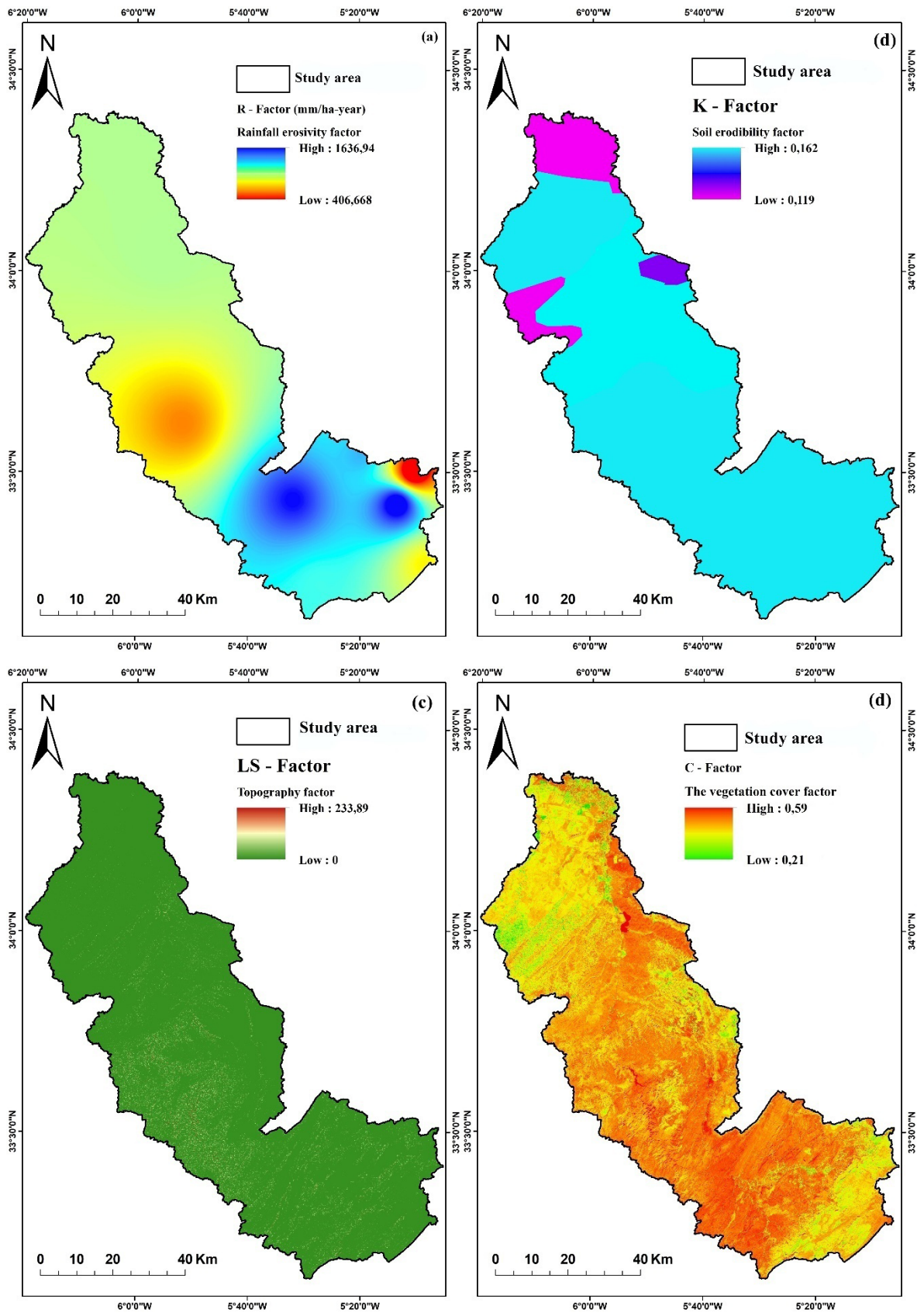


Figure 5. Factors controlling soil erosion in the Ouljet Sultane watershed: (a) rainfall erosivity (R); (b) soil erodibility factor (K); (c) topographic factor (LS); (d) cover management factor (C).

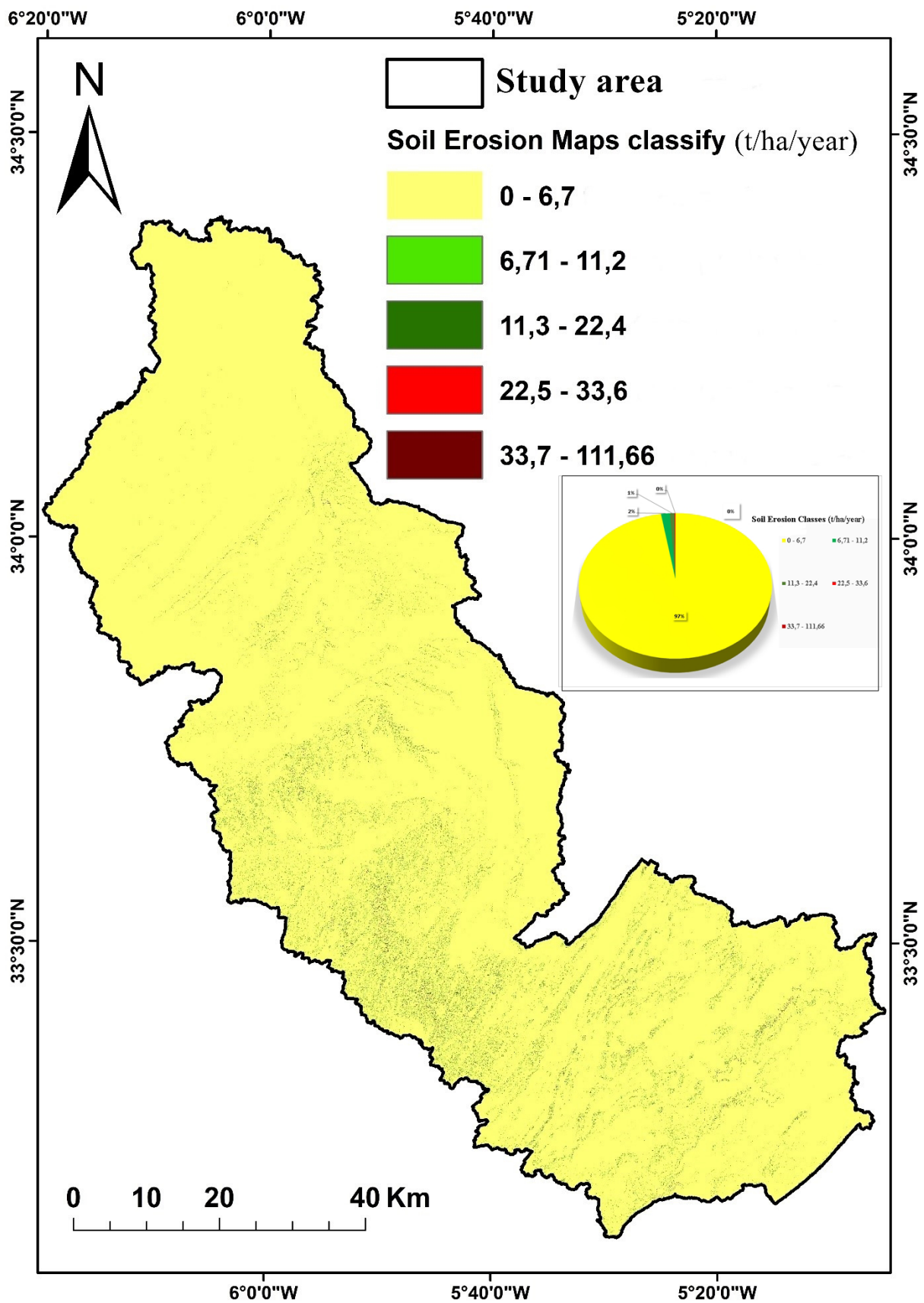


Figure 6. Categories of erosion risk and their spatial distribution in the study area.

DISCUSSION

The results of this study reveal significant insights into the spatial distribution of soil erosion risk within Ouljet Sultane watershed, particularly highlighting the predominance of low erosion values across the area (Fig.7). According to the findings, approximately 97% of the study region exhibits low erosion rates, as illustrated in Figure 7. This raises important considerations regarding the local environmental conditions and the factors influencing these outcomes. The low erosion values can be attributed to several key factors inherent to the watershed's characteristics. Firstly, the rainfall erosivity (R) factor, which varies significantly across the region, indicates that while certain areas experience intense rainfall events, much of the watershed maintains relatively moderate precipitation patterns. This variability contributes to the overall lower erosion rates observed. The spatial distribution of rainfall, coupled with the terrain's topography, further influences runoff dynamics, which are crucial in erosion processes. Additionally, the soil erodibility (K) factor plays a critical role in determining erosion susceptibility. The data used in this study indicate that the majority of soils in the watershed possess properties that enhance their resistance to erosion. Factors such as high permeability and organic matter content contribute to this resilience, allowing soils to absorb rainfall effectively and reduce surface runoff. Areas with lower K values are particularly noteworthy, as they indicate soils that are less prone to detachment and transport, thus supporting the observed low erosion rates. Topography, represented by the slope length and steepness (LS) factor, also influences erosion dynamics. The majority of the watershed comprises gentle slopes, which limit the velocity of water flow and reduce the potential for erosion. In contrast, only a small fraction of the area is characterized by steep gradients, where erosion risk is inherently higher. The combination of

these topographic features contributes to the overall stability of the landscape.

Moreover, the cover management factor (C) reflects the impact of vegetation and land use practices on erosion control. The presence of vegetation, whether from natural shrubland or agricultural practices, plays a significant role in protecting soil surfaces from the erosive forces of rainfall. In our study, areas with robust vegetation cover exhibited markedly lower erosion rates, reaffirming the importance of effective land management strategies. In contrast, the limited areas that showed higher erosion values warrant further investigation. These zones may be subjected to localized factors such as deforestation, poor agricultural practices, or concentrated runoff from impervious surfaces. Understanding the specific conditions that lead to elevated erosion risk in these pockets is crucial for developing targeted conservation measures.

The potential for water erosion risk in several basins in Morocco has been investigated at the national level, with different degrees of soil loss depending on the location. According to the literature, researchers have reported varying rates of soil erosion in several watersheds and basins in Morocco. In the northwest Rif area, the average annual erosion rates were found 47.18 t/h in the Oued Sania basin and 34.74 t/h in the Kalaya basin (Tahiri *et al.* 2015, 2017). According to Ouallali *et al.* (2016), the average annual erosion rate in the Arbaa Ayacha River watershed within the western Rif region was determined to be 25 t/ha. The Oued Salha watershed in the central Rif had a greater rate of soil loss at 55.53 t/ha annually than the Oued Boussouab watershed in the eastern Rif, which saw an annual loss of about 22 t/ha/year (Sadiki *et al.* 2007). Oued Inaouene watershed in the Prerif was estimated to have an erosion rate of 36.33 t/h/y (Benzougagh *et al.* 2021, 2024).

In the Bouregreg watershed, the specific erosion rates, estimated according to the USLE and RUSLE models, are



Figure 7. Various expressions of the issue of water erosion in the research region.

respectively 0.94 (t/ha/year), 1.07 (t/ha/year) (Hara *et al.* 2021). The estimated rates of erosion for the Oum Er-Rbia watershed in the Middle Atlas varied greatly, ranging from 58 t/h/y (El Jazouli *et al.* 2019) to 224 t/h/y (Yjjou *et al.* 2014). An estimate of the soil loss in the Sebou watershed, which makes up more than 70% of the Gharb area, was 10 t/ha/year (Chadli 2016). Ultimately, it was estimated that the N'fis watershed in the western High Atlas would have a higher rate of 115 t/h/y, whereas the Haouz plain in the High Atlas had a significantly lower average annual soil erosion rate of 3.53 t/h/y (Markhi *et al.* 2019, Bammou *et al.* 2024).

Conclusion and recommendations

This study focused on predicting soil erosion risk in relation to land use within the Ouljet Sultane watershed. The findings indicate that land use is a major controlling factor in triggering both surface and deep erosion. The relationship between erosion and various causative parameters is characterized by significant spatial heterogeneity. This heterogeneity is explained by the wide variety of land use classes, which are themselves influenced by factors such as water action, lithology, geomorphological context, and human interventions.

The results highlight central Morocco as a highly vulnerable and fragile area, where erosion and other forms of slope instability are exacerbated by increasing anthropogenic pressure. In this region, the current evolution of slopes is driven by highly active instability, with diverse forms and processes. The uneven distribution of these forms across space and time reflects the varying sensitivity of different environments and implicates multiple factors of both natural and human origin.

Anthropogenic activity, which has intensified over the last decade, is a key driver of landslides and the development of badlands. This situation should prompt decision-makers to accompany their infrastructure and urban development projects with preventive measures aimed at ensuring the hydrological and gravitational stabilization of slopes.

Soil erosion is a major global issue, particularly affecting agricultural communities. In light of the study area's vulnerability to climate change, it is essential to assess the impact of erosion on land degradation. This knowledge will empower decision-makers and land managers to implement appropriate conservation and protection measures. Examining the geographical distribution of soil erosion in the Ouljet Sultane watershed is the aim of this study. Legislators and land use/cover planners may utilize the generated data to guide policy-level planning processes for conservation and management, offering crucial information for environmentally friendly and sustainable land use practices. Based on the integration of many RUSLE model variables processed via GIS software, the study's findings. The study predicts an average of 22.5 tons of soil erosion loss per acre each year. The findings of this study emphasize the need for a holistic and economically viable approach to soil protection, especially in regions susceptible to erosion.

Increasing the amount of vegetative cover on the land is the most crucial aspect of conservation, and farmers, or the local population, should be involved in all conservation efforts. The most vulnerable characteristics (management variables) that cause soil erosion should be evaluated under various management scenarios improve conservation planning. Future research should also examine how agricultural productivity is affected by soil loss; How can soil sustainability be ensured over the long term? How can farmers get ready for water

conservation? The study's findings would make it easier to see how land uses and a watershed's risk of erosion are related, allowing the conclusions to be applied to other watersheds with comparable landforms, soil types, and land use/land cover.

Conflicts of Interest: The authors declare no conflicts of interest.

Acknowledgments

The authors would like to express their gratitude to the editor of «Bulletin de l'Institut Scientifique» ACHAB Mohammed and the anonymous journal reviewers for their significant contribution to the improvement of the manuscript.

REFERENCES

- Ait Yacine E., Oudija F., Nassiri L. *et al.* 2019. Modélisation et Cartographie des Risques d'érosion Hydrique du Sol par l'application des SIG, Télédétecton et Directives PAP/CAR. Cas du Bassin Versant de Beht, Maroc. *European Scientific Journal*, 15(12), 1857-7431. <http://dx.doi.org/10.19044/esj.2019.v15n12p259>.
- Arnold J.G., Moriasi D.N., Gassman P.W. *et al.* 2012. SWAT: Model use, calibration, and validation. *Transactions of the ASABE*, 55(4), 1491-1508. <https://doi.org/10.13031/2013.42256>.
- Arsyad S. 2010. Konservasi Tanah dan Air. *IPB Press*. Bogor, 396 p.
- Bammou Y., Brahim B., Abdessalam O. *et al.* 2024. Machine learning models for gully erosion susceptibility assessment in the Tensift catchment, Haouz Plain, Morocco for sustainable development. *Journal of African Earth Sciences*, 105229. <https://doi.org/10.1016/j.jafrearsci.2024.105229>.
- Bammou Y., Benzougagh B., Bensaid A. *et al.* 2024. Mapping of current and future soil erosion risk in a semi-arid context (haouz plain-Marrakech) based on CMIP6 climate models, the analytical hierarchy process (AHP) and RUSLE. *Modeling Earth Systems and Environment*, 10(1), 1501-1514. <https://doi.org/10.1007/s40808-023-01845-9>.
- Batista P.V., Davies J., Silva M.L. *et al.* 2019. On the evaluation of soil erosion models : Are we doing enough?. *Earth-Science Reviews*, 197, 102898. <https://doi.org/10.1016/j.earscirev.2019.102898>.
- Beaudet G. 1969. *Le plateau central marocain et ses bordures, étude géomorphologique*. Thèse de Doctorat, Paris I, 478 p.
- Benkobi L., Trlica M. J., & Smith J. L. 1994. Evaluation of a refined surface cover subfactor for use in RUSLE. *Journal of Range Management*, 47(1), 74-78.
- Benzougagh B., Frison P.L., Meshram S.G. *et al.* 2021. Flood Mapping Using Multi-Temporal Sentinel-1 SAR Images: A Case Study—Inaouene Watershed from Northeast of Morocco. *Iranian Journal of Science and Technology, Transactions of Civil Engineering*, 1-10. <https://doi.org/10.1007/s40996-021-00683-y>.
- Benzougagh B., Meshram S.G., Dridri A. *et al.* 2022. Identification of critical watershed at risk of soil erosion using morphometric and geographic information system analysis. *Applied Water Science*, 12, 1-20. <https://doi.org/10.1007/s13201-021-01532-z>.
- Benzougagh B., Meshram S.G., Fellah B.E. *et al.* 2023. Mapping of land degradation using spectral angle mapper approach (SAM): the case of Inaouene watershed (Northeast Morocco). *Modeling Earth Systems and Environment*, 1-11. <https://doi.org/10.1007/s40808-023-01711-8>.
- Benzougagh B., Al-Quraishi A. M. F., Bammou Y. *et al.* 2024. Spectral Angle Mapper Approach (SAM) for Land Degradation Mapping: A Case Study of the Oued Lahdar Watershed in the

- Pre-Rif Region (Morocco). In *Natural Resources Deterioration in MENA Region: Land Degradation, Soil Erosion, and Desertification*. Cham: Springer International Publishing, 15-35. https://doi.org/10.1007/978-3-031-58315-5_2.
- Bezak N., Borrelli P., Mikoš M. *et al.* 2024. Towards multi-model soil erosion modelling : An evaluation of the erosion potential method (EPM) for global soil erosion assessments. *Catena*, 234, 107596. <https://doi.org/10.1016/j.catena.2023.107596>.
- Brahim B., Meshram S.G., Abdallah D. *et al.* 2020. Mapping of soil sensitivity to water erosion by RUSLE model: case of the Inaouene watershed (Northeast Morocco). *Arabian Journal of Geosciences*, 13, 1-15. <https://doi.org/10.1007/s12517-020-06079-y>.
- Capella W., Hernández-Molina F.J., Flecker R. *et al.* 2017. Sandy contourite drift in the late Miocene Rifian Corridor (Morocco): reconstruction of depositional environments in a foreland-basin seaway. *Sedimentary Geology*, 355, 31-57. <https://doi.org/10.1016/j.sedgeo.2017.04.004>.
- Cerdan O., Souchère V., Lecomte V. *et al.* 2002. Incorporating soil surface crusting processes in an expert-based runoff model: Sealing and Transfer by Runoff and Erosion related to Agricultural Management. *Catena*, 46(2-3), 189-205. [https://doi.org/10.1016/S0341-8162\(01\)00166-7](https://doi.org/10.1016/S0341-8162(01)00166-7).
- Chadli K. 2016. Estimation of soil loss using RUSLE model for Sebou watershed (Morocco). *Modeling Earth Systems and Environment*, 2, 1-10. <https://doi.org/10.1007/s40808-016-0105-y>.
- da Silva A.M. 2004. Rainfall erosivity map for Brazil. *Catena*, 57(3), 251-259. <https://doi.org/10.1016/j.catena.2003.11.006>.
- Dutta D., Routray A., Preveen Kumar D. *et al.* 2019. Simulation of a heavy rainfall event during southwest monsoon using high-resolution NCUM-modeling system: a case study. *Meteorology and Atmospheric Physics*, 131, 1035-1054. <https://doi.org/10.1007/s00703-018-0619-0>.
- El Brahim M., Brahim B. & Najia F. 2022. Quantification of Soil Sensitivity to Water Erosion by the RUSLE Model in the Oued Amter Watershed, NorthWestern Morocco. *The Iraqi Geological Journal*, 41-56. <https://doi.org/10.46717/igj.55.2C.4ms-2022-08-17>.
- El Jazouli A., Barakat A., Khellouk R. *et al.* 2019. Remote sensing and GIS techniques for prediction of land use land cover change effects on soil erosion in the high basin of the Oum Er Rbia River (Morocco). *Remote Sensing Applications: Society and Environment*, 13, 361-374. <https://doi.org/10.1016/j.rsase.2018.12.004>.
- Ezzaoui M.A., Mahé G., Kacimi I. *et al.* 2020. Comparison of the MUSLE Model and Two Years of Solid Transport Measurement, in the Bouregreg Basin, and Impact on the Sedimentation in the Sidi Mohamed Ben Abdellah Reservoir, Morocco. *Water*, 12(7), 1882. doi:<https://doi.org/10.3390/w12071882>.
- Faouzi E., Arioua A., Namous M. *et al.* 2023. Spatial mapping of hydrologic soil groups using machine learning in the Mediterranean region. *Catena*, 232, 107364. <https://doi.org/10.1016/j.catena.2023.107364>.
- Fedan B. 1988. Evolution géodynamique d'un bassin intraplaque sur décrochements : le moyen atlas (Maroc) durant le méso-cénozoïque. Travaux de l'Institut scientifique. Série géologie et géographie physique, 17, 337p.
- Fu B., Liu Y., Lü Y. *et al.* 2011. Assessing the soil erosion control service of ecosystems change in the Loess Plateau of China. *Ecological Complexity*, 8(4), 284-293. <https://doi.org/10.1016/j.ecocom.2011.07.003>.
- Ganasri B. & Ramesh H. 2016. Assessment of soil erosion by RUSLE model using remote sensing and GIS-A case study of Nethravathi Basin. *Geoscience Frontiers*, 7(6), 953-961. <https://doi.org/10.1016/j.gsf.2015.10.007>.
- Ganzour S.K., Aboukoto M.E.S., Hassaballa H. *et al.* 2024. Land Degradation, Desertification & Environmental Sensitivity to Climate Change in Alexandria and Beheira, Egypt. *Egyptian Journal of Soil Science*, 64(1). <https://doi.org/10.21608/ejss.2023.237386.1664>.
- Gavrilovic S. 1962. Important References to Exploration, Science, Technology, and Hispanic American History in Yugoslav Archives. In *Proceedings of the Pennsylvania Academy of Science*. *Pennsylvania Academy of Scienc.*, 22-29.
- Haan C.T., Barfield B.J. & Hayes J.C. 1994. Design hydrology and sedimentology for small catchments. *Elsevier*.
- Hara F., Achab M., Emran A. *et al.* 2021. Quantification of water erosion using USLE and RUSLE methods: Application to the Bouregreg sub-watersheds, Morocco. *Bulletin de l'Institut Scientifique Rabat section Sciences de la Terre*, 4, 69-87.
- Jahun B.G., Ibrahim R., Dlamini N.S. *et al.* 2015. Review of soil erosion assessment using RUSLE model and GIS. *Journal of Biology, Agriculture and Healthcare*, 5(9), 36-47.
- Karydas C.G., Panagos P. & Gitas I.Z. 2014. A classification of water erosion models according to their geospatial characteristics. *International Journal of Digital Earth*, 7(3), 229-250. <https://doi.org/10.1080/17538947.2012.671380>.
- Karydas C., Panagos P. 2020. Towards an assessment of the ephemeral gully erosion potential in Greece using Google Earth. *Water*, 12(2), 603. <https://doi.org/10.3390/w12020603>.
- Khali Issa L., Ben Hamman Lech-Hab K., Raïssouni A. *et al.* 2016. Cartographie quantitative du risque d'érosion des sols par approche SIG/USLE au niveau du bassin versant Kalaya (Maroc Nord Occidental). *Journal of Materials and Environmental Scienc*, 7, 2778-2795.
- Kriegler F.J. 1969. Preprocessing transformations and their effects on multispectral recognition. In *Proceedings of the Sixth International Symposium on Remote Sensing of Environmen*, 97-13.
- Laabidi A., Gourari L., Hmaid A. *et al.* 2017. Recent deposits of dejection cones and of the flood plain of the valley of Middle Beht River (South Rif corridor, Morocco): Sedimentology and environmental study. *Journal of Materials and Environmental Science*, 8(9), 3313-3325.
- Lakhili F., Chaouan J., Qadem Z. *et al.* 2021. GIS based soil erosion estimation using EPM method in the Beht catchment. *VEWASH & TI Journal*, 5(2), 588-596.
- Lakhili F. 2018. *Evaluation de la qualité des eaux et des sédiments et cartographiede l'érosion hydrique dans le bassin versant du haut Beht*. Thèse de doctorat, Université Sidi Mohamed Ben Abdellah, Faculté des Sciences et technique, 234p.
- Lee S. 2004. Soil erosion assessment and its verification using the universal soil loss equation and geographic information system: a case study at Boun, Korea. *Environmental Geology*, 45, 457-465. <https://doi.org/10.1007/s00254-003-0897-8>.
- Marghich A. 1988. *Contribution à l'étude sédimentologique, minéralogique et géochimique des alluvions actuelles de l'oued Beht (Maroc Central)*. Thèse de 3ème cycle, Ecole Normale Supérieur, 256 p.
- Markhi A., Laftouhi N., Grusson Y. *et al.* 2019. Assessment of potential soil erosion and sediment yield in the semi-arid N'fis

- basin (High Atlas, Morocco) using the SWAT model. *Acta Geophysica*, 67, 263-272. <https://doi.org/10.1007/s11600-019-00251-z>.
- Mastere M., Van-Vliet Lanoë B., Ait Brahim L. 2013. Cartographie de l'occupation des sols en relation avec les mouvements gravitaires et le ravinement dans le Rif nord-occidental (Maroc). *Géomorphologie: relief, processus, environnement*, 19(3), 335-352. doi: <https://doi.org/10.4000/geomorphologie.10328>.
- Mastere M. 2011. *L'aléa mouvements de terrain dans la province de Chefchaouen (Rif Central, Maroc): Analyse Spatiale, et Modélisation Probabiliste Multi-Echelle*. These de Doctorat, Université Européenne de Bretagne, 314p.
- Mastere M. 2020a. Mass movement hazard assessment at a medium scale using weight of evidence model and neo-predictive variables creation. *Advances in Science, Technology and Innovation*, 73-85. DOI 10.1007/978-3-030-21166-0_7.
- Mastere M., Achbun A. & El Fellah B. 2020b. Open Remote Sensing Image Classification Using NDVI and Thermal Bands. *Advances in Science, Technology and Innovation*, 149-161. DOI10.1007/978-3-030-21166-0_13.
- Mastere M., El Fellah B. & Maquaire O. 2020c. Landslides inventory map as a first step for hazard and risk assessment: Rif mountains, Morocco. *Bulletin de l'institut Scientifique, Rabat, Section Sciences de la Terre*, 42, 49-62.
- Mccool D.K., Brown L.C., Foster G.R. *et al.* 1987. Revised slope steepness factor for the Universal Soil Loss Equation. *Transactions of the ASAE*, 30(5), 1387-1396. <https://doi.org/10.13031/2013.30576>.
- Michard A. 1976. Eléments de géologie marocaine. *Notes et mémoires du service géologique, N° 252*, 408 p.
- Millward A.A., Mersey J.E. 1999. Adapting the RUSLE to model soil erosion potential in a mountainous tropical watershed. *Catena*, 38(2), 109-129. [https://doi.org/10.1016/S0341-8162\(99\)00067-3](https://doi.org/10.1016/S0341-8162(99)00067-3).
- Morgan R.P.C., Morgan D.D.V. & Finney H.J. 1984. A predictive model for the assessment of soil erosion risk. *Journal of agricultural engineering research*, 30, 245-253. [https://doi.org/10.1016/S0021-8634\(84\)80025-6](https://doi.org/10.1016/S0021-8634(84)80025-6).
- Morgan R.P.C. 2001. A simple approach to soil loss prediction: a revised Morgan–Morgan–Finney model. *Catena*, 44(4), 305-322. [https://doi.org/10.1016/S0341-8162\(00\)00171-5](https://doi.org/10.1016/S0341-8162(00)00171-5).
- Moussi R., Bengamra S., Bouziane H. *et al.* 2023. Quantification of soil erosion by USLE model in the Oued Za watershed (Northeastern Morocco) – Quantification de l'érosion des sols par le modèle USLE dans le bassin versant de l'Oued Za (Nord-Est du Maroc). *Bulletin de l'Institut Scientifique, Rabat, Section Sciences de la Terre*, 2023, 45, 83–96.
- Nastos P.T., Kapsomenakis J. & Douvis K.C. 2013. Analysis of precipitation extremes based on satellite and high-resolution gridded data set over Mediterranean basin. *Atmospheric Research*, 131, 46-59. <https://doi.org/10.1016/j.atmosres.2013.04.009>.
- Nearing M.A., Norton L.D., Bulgakov D.A. *et al.* 1997. Hydraulics and erosion in eroding rills. *Water Resources Research*, 33(4), 865-876. <https://doi.org/10.1029/97WR00013>.
- Ouallali A., Moukhchane M., Aassoumi H. *et al.* 2016. Evaluation and mapping of water erosion rates in the watershed of the ArbaaAyacha River (Western Rif, Northern Morocco). *Bulletin de l'Institut Scientifique, Section Sciences de la Terre*, 38, 65–79.
- Ollobarren Del Barrio P., Campo-Bescos M.A., Gimenez R. *et al.* 2018. Assessment of soil factors controlling ephemeral gully erosion on agricultural fields. *Earth Surf. Process. Landforms* 43 (9), 1993–2008.
- Osman K.T. & Osman K.T. 2014. Soil erosion by water. *Soil degradation, conservation and remediation*, 69-101. https://doi.org/10.1007/978-94-007-7590-9_3.
- Phinzi K., Abriha D. & Szabó S. 2021. Classification efficacy using k-fold cross-validation and bootstrapping resampling techniques on the example of mapping complex gully systems. *Remote Sensing*, 13(15), 2980. <https://doi.org/10.3390/rs13152980>.
- Prakash C. & Nagarajan R. 2017. Outburst susceptibility assessment of moraine-dammed lakes in Western Himalaya using an analytic hierarchy process. *Earth surface processes and landforms*, 42(14), 2306-2321. <https://doi.org/10.1002/esp.4185>.
- Renard K.G., Foster G.R., Weesies G.A. *et al.* 1991a. Predicting soil erosion by water a guide to conservation planning with the Revised Universal soil Loss Equation (RUSLE). Report ARS-703, US Dept Agric. *Agricultural Research Service*.
- Renard K.G. & Freimund J.R. 1994. Using monthly precipitation data to estimate the R-factor in the revised USLE. *Journal of hydrology*, 157(1-4), 287-306. [https://doi.org/10.1016/0022-1694\(94\)90110-4](https://doi.org/10.1016/0022-1694(94)90110-4).
- Renard K.G., Meyer L.D. & Foster G.R. 1997. Introduction and history. Predicting soil erosion by water: a guide to conservation, planning with the revised universal soil loss equation (RUSLE), 2-18.
- Römkens M.J.M., Luk S.H., Poesen J.W.A. *et al.* 1995. Rain infiltration into loess soils from different geographic regions. *Catena*, 25(1-4), 21-32. [https://doi.org/10.1016/0341-8162\(94\)00039-H](https://doi.org/10.1016/0341-8162(94)00039-H).
- Sabaoui A. 1987. *Structure et évolution alpine du Moyen-Atlas Septentrional sur la transversale Tleta des Zerarda-Meghraoua (SW de Taza, Maroc)*. Thèse de 3^{ème} cycle, Université Paul Sabatier, Toulouse III, 162 p.
- Sadiki A., Faleh A., Navas A. *et al.* 2007. Assessing soil erosion and control factors by the radiometric technique in the Boussouab catchment, Eastern Rif, Morocco. *Catena*, 71(1), 13-20. <https://doi.org/10.1016/j.catena.2006.10.003>.
- Sadiki A., Faleh A., Zêzere J.L. *et al.* 2009. Quantification de l'Erosion en Nappes dans le Bassin Versant de l'Oued Sahla-Rif Central Maroc. *Cahiers géographiques*, 6, 59-70.
- Sadkaoui D., Benzougagh B., Afaf A. *et al.* 2023. Mapping of Zones Vulnerable to Water Erosion Using PAP/CAR and GIS Method Upper the Aït Moulay Hmad Dam, Northeast of the Central Massif, Morocco. *The Iraqi Geological Journal*, 181-197. <https://doi.org/10.46717/igj.56.1B.14ms-2023-2-22>.
- Saidi A., Bouramtane T., Achab M. *et al.* 2020. The Hough transform algorithm coupled with spatial filtering for the study of geological structuring control on the drainage network : application to the North Oulmes region, Morocco. *Arabian Journal of Geosciences*, 13, 1-17. <https://doi.org/10.1007/s12517-020-06052-9>.
- Sands P. 2023. Environmental protection in the twenty-first century: sustainable development and international law. *In The global environment*, 116-137.
- Šarapatka B., Alvarado-Solano D.P. & Čizmar D. 2019. Can glomalin content be used as an indicator for erosion damage to soil and related changes in organic matter characteristics and nutrients? *Catena*, 181, 104078. <https://doi.org/10.1016/j.catena.2019.104078>.
- Shamshad A., Leow C.S., Ramlah A. *et al.* 2008. Applications of AnnAGNPS model for soil loss estimation and nutrient loading for Malaysian conditions. *International Journal of Applied*

- Earth Observation and Geoinformation*, 10(3), 239-252. <https://doi.org/10.1016/j.jag.2007.10.006>.
- Shi Z.H., Fang N.F., Wu F.Z. *et al.* 2012. Soil erosion processes and sediment sorting associated with transport mechanisms on steep slopes. *Journal of Hydrology*, 454, 123-130. <https://doi.org/10.1016/j.jhydrol.2012.06.004>.
- Stone RP., Hilborn D. 2012. Universal soil loss equation (USLE) factsheet. *Ministry of Agriculture, Food and Rural Affairs, Ontario*.
- Tahiri M., Tabyaoui H., Tahiri A. *et al.* 2015. Modelling soil erosion and sedimentation in the Oued Haricha sub-basin (Tahaddart watershed, Western Rif, Morocco): risk assessment. *Journal of Geoscience and Environment Protection*, 4(1), 107-119. <https://doi.org/10.4236/gep.2016.41013>.
- Tahiri M., Tabyaoui H., El Hammichi F. *et al.* 2017. Quantification de l'érosion hydrique et de la sédimentation à partir de modèles empiriques dans le bassin versant de Tahaddart (Rif nord occidental, Maroc). *Bulletin de l'Institut Scientifique, Rabat, Section Sciences de la Terre*, 39, , 87-101.
- Van Oost K., Govers G., Desmet P. *et al.* 2000. Evaluating the effects of changes in landscape structure on soil erosion by water and tillage. *Landscape ecology*, 15, 577-589. <https://doi.org/10.1023/A:1008198215674>.
- Wischmeier W. H., Smith D.D. 1965. Predicting rainfall-erosion losses from cropland east of the Rocky Mountains: Guide for selection of practices for soil and water conservation (No. 282). *Agricultural Research Service, US Department of Agriculture*.
- Wischmeier W.H., Smith D.D. 1978. Predicting rainfall erosion losses: a guide to conservation planning (No. 537). *Department of Agriculture, Science and Education Administration*.
- Yjjou M., Bouabid R., El Hmaidi A. *et al.* 2014. Modélisation de l'érosion hydrique via les SIG et l'équation universelle des pertes en sol au niveau du bassin versant de l'Oum Er-Rbia. *The International Journal of Engineering and Science*, 3(8), 83-91.
- Yitayew M., Pokrzywka S.J. & Renard K.G. 1999. Using GIS for facilitating erosion estimation. *Applied Engineering in Agriculture*, 15(4), 295-301. <https://doi.org/10.13031/2013.5780>.
- Yuan Z., Chu Y. & Shen Y. 2015. Simulation of surface runoff and sediment yield under different land-use in a Taihang Mountains watershed, North China. *Soil and Tillage Research*, 153, 7-19. <https://doi.org/10.1016/j.still.2015.04.006>.

Manuscrit reçu le 04/07/2024
Version révisée acceptée le 13/01/2025
Version finale reçue le 06/03/2025
Mise en ligne le 09/04/2025